Iik Bhakti Wiyata Kediri Perpustakaan 1

Modification of Zn-Metal Organic Framework with Nano Silver as an Antibacterial Material for Diabetic Ulcers (in vitro)

PERPUSTAKAAN 8
Perpustakaan
Institut Ilmu Kesehatan Bhakti Wiyata Kediri

Document Details

Submission ID
trn:oid:::1:3018540757

Submission Date
Sep 24, 2024, 9:39 AM GMT+7

Download Date
Sep 25, 2024, 7:32 AM GMT+7

File Name
0._RJPT_Mama_Dapus_2_2_2_-_Fery_Pujiono.docx

File Size
4.2 MB

13 Pages

7,170 Words

41,363 Characters

13% Overall Similarity

The combined total of all matches, including overlapping sources, for each database.

Filtered from the Report

- Bibliography
- Quoted Text

Exclusions

- 62 Excluded Matches

Match Groups

83 Not Cited or Quoted 13%
Matches with neither in-text citation nor quotation marks

0 Missing Quotations 0%
Matches that are still very similar to source material

0 Missing Citation 0%
Matches that have quotation marks, but no in-text citation

0 Cited and Quoted 0%
Matches with in-text citation present, but no quotation marks

Top Sources

9% Internet sources
11% Publications
1% Submitted works (Student Papers)

Integrity Flags

1 Integrity Flag for Review

Replaced Characters
24 suspect characters on 6 pages
Letters are swapped with similar characters from another alphabet.

Our system's algorithms look deeply at a document for any inconsistencies that would set it apart from a normal submission. If we notice something strange, we flag it for you to review.

A Flag is not necessarily an indicator of a problem. However, we'd recommend you focus your attention there for further review.

Match Groups

- **83** Not Cited or Quoted 13%
  Matches with neither in-text citation nor quotation marks
- **0** Missing Quotations 0%
  Matches that are still very similar to source material
- **0** Missing Citation 0%
  Matches that have quotation marks, but no in-text citation
- **0** Cited and Quoted 0%
  Matches with in-text citation present, but no quotation marks

Top Sources

9% Internet sources
11% Publications
1% Submitted works (Student Papers)

Top Sources

The sources with the highest number of matches within the submission. Overlapping sources will not be displayed.

1	Publication	Sima Kalhor, Hassan Sepehrmansourie, Mahmoud Zarei, Mohammad Ali Zolfigol, ...	1%
2	Internet	repository.futminna.edu.ng:8080	1%
3	Publication	Ya-Meng Wu, Pei-Chen Zhao, Bin Jia, Zhe Li, Shuai Yuan, Cheng-Hui Li. "A silver-fu...	1%
4	Publication	Shu-Fang Zhou, Guo-Mei Wu, Chen-Xi Zhang, Qing-Lun Wang. "Significant Enhanc...	0%
5	Internet	www.mdpi.com	0%
6	Internet	link.springer.com	0%
7	Internet	www.researchgate.net	0%
8	Publication	Shen Hu, Min Liu, Keyan Li, Chunshan Song, Guoliang Zhang, Xinwen Guo. " Surfa...	0%
9	Publication	M. Fatahi Bafghi, S. Salary, F. Mirzaei, H. Mahmoodian, H. Meftahizade, R. Zaresha...	0%
10	Internet	auctoresonline.org	0%

11 Internet
www.nanomedicine-rj.com 0%

12 Publication
Benaidja Yasmina, Bounoukta Charf Eddine, Fenni Manel, Sid Dounia, Bezzi Hamz... 0%

13 Internet
kipdf.com 0%

14 Internet
www.frontiersin.org 0%

15 Publication
Ramalingam, Anantharaj, and Jegalakshimi Jewaratnam. "Simultaneous interacti... 0%

16 Internet
worldwidescience.org 0%

17 Internet
d.researchbib.com 0%

18 Publication
Ram K. Gupta, Tahir Rasheed, Tuan Anh Nguyen, Muhammad Bilal. "Metal-Organi... 0%

19 Internet
pubmed.ncbi.nlm.nih.gov 0%

20 Publication
Yinchun Hu, Hui Yang, Renhu Wang, Menglan Duan. "Fabricating Ag@MOF-5 nan... 0%

21 Internet
e-journal.unair.ac.id 0%

22 Publication
Andrés Santarelli, Cândida A. Brandl, Camila N. Cechin, Tanize Bortolotto et al. "N... 0%

23 Publication
M.J Van Stipdonk, S.L von Heimburg, E.A Schweikert. "Probing silicon substitution ... 0%

24 Publication
Malihe Zeraati, Mohammadreza Moghaddam-Manesh, Sepideh Khodamoradi, Sar... 0%

25 Internet
www.ncbi.nlm.nih.gov 0%

26 Internet
www.nctimes.com 0%

27 Publication
Rebaz F. Hamarawf. "Antibacterial, antibiofilm, and antioxidant activities of two n... 0%

28 Student papers
The University of Manchester 0%

29 Publication
Ton Duc Thang University 0%

30 Internet
journals.plos.org 0%

31 Internet
www.nepjol.info 0%

32 Internet
www.science.gov 0%

33 Publication
Bibhuti Bhusan Rath, Jagadese J. Vittal. "Water Stable Zn(II) Metal–Organic Frame... 0%

34 Publication
Dini Assyfa, Marlina Marlina, Akmal Djamaan. "MSC Secretome's Antibacterial Act... 0%

35 Publication
M. A. Diab, A. Z. El-Sonbati, D. M. D. Bader, M. Sh. Zoromba. "Thermal Stability and... 0%

36 Publication
M. López-R, Yue Barrios, Leon D. Perez, CY. Soto, C. Sierra. "Metal-Organic Frame... 0%

37 Internet
hdl.handle.net 0%

38 Internet
jcpr.or.kr 0%

39 Internet
utpedia.utp.edu.my 0%

40 Internet
www.dovepress.com 0%

41 Publication
Douchao Mei, Lijia Liu, Huan Li, Yudan Wang, Fuqiu Ma, Chunhong Zhang, Hongxi... 0%

42 Publication
Himanshi Gupta, Isha Saini, Vinamrita Singh, Varsha Singh, Bikash Mishra. "Enha... 0%

43 Publication
Hossein Shahriyari Far, Mahdi Hasanzadeh, Mohammad Shabani Nashtaei, Mahb... 0%

44 Publication
Ifeoluwaposi Oluwabunmi Ogundana, Adewale Oluwasogo Olalemi, Daniel Juwon... 0%

45 Publication
Selene Berni, Demetrio Scelta, Samuele Fanetti, Roberto Bini. "High Pressure Beh... 0%

46 Publication
Tingting Chen, Yunchuan Jiang, Yinbing Wu, Meilin Lai et al. "Doughnut-shaped bi... 0%

47 Internet
discovery.researcher.life 0%

48 Internet
pubblicazioni.unicam.it 0%

49 Internet
www.aak.gov.az 0%

50 Internet
www.ajtmh.org 0%

51 Internet
www.nature.com 0%

52 Internet
www.preprints.org 0%

53 Publication

Haoyang Xu, Pengbiao Geng, Wanchang Feng, Meng Du, Dae Joon Kang, Huan Pa... 0%

54 Publication

Sheeba Khan, Prasenjit Das, Sanjay K. Mandal. " Design and Construction of a Lu... 0%

55 Publication

Yoon-moon Chun, Peter Claisse, Tarun R. Naik, Eshmaiel Ganjian. "Sustainable Co... 0%

56 Internet

ajcmi.umsha.ac.ir 0%

57 Publication

"Metal-Organic Frameworks (MOFs) as Catalysts", Springer Science and Business ... 0%

58 Publication

B. Shivaleela, G.G. Shivraj, S.M. Hanagodimath. "Estimation of dipole moments by... 0%

59 Internet

www.hindawi.com 0%

Type of Manuscript:
Research

Modification of Zn-Metal Organic Framework with Nano Silver as an Antibacterial Material for Diabetic Ulcers *(in vitro)*

Tri Ana Mulyati[1*], Juni Ekowati[2], Yohanes Andy Rias[3], Binti Mu'arofah[4], Fery Eko Pujiono[1]

[1] Departement of Pharmacy, Institut Ilmu Kesehatan Bhakti Wiyata, Kediri, Indonesia
[2] Departement of Pharmaceutical, Airlangga University, Surabaya, Indonesia
[3] Departement of Nursing, Institut Ilmu Kesehatan Bhakti Wiyata, Kediri, Indonesia
[4] Departement of Medical Laboratory Technology, Institut Ilmu Kesehatan Bhakti Wiyata, Kediri, Indonesia.

*Corresponding author:
Department of Pharmacy,
Institut Ilmu Kesehatan Bhakti Wiyata,
Jl. KH. Wachid Hasyim 65, Kediri, Indonesia.
E-mail address: nanapujiono@gmail.com

ABSTRACT:

Zn-MOF synthesis was carried out using the solvothermal method with DMF as the solvent, and Zn-MOF was modified with AgNPs to produce Ag/Zn-MOF using ultrasonication. XRD analysis results indicate that Ag(10)/Zn-MOF and Ag(20)/Zn-MOF exhibit diffraction patterns similar to Zn-MOF but with some shifts and the addition of new peaks at 2θ around 38º and 45º, characteristic of Ag_2O and AgO. FTIR analysis confirms the successful synthesis of Zn-MOF, as evidenced by characteristic functional group vibrations observed in the ATR-FTIR spectrum, such as $-COO_{sym}$ (1584 cm^{-1}) and $-COO_{asym}$ (1393 cm^{-1}), indicating the bonding between carboxylate ligands and the central Zn metal, as well as Zn-O vibration (646 cm^{-1}), indicating the presence of Zn_4O metal clusters. After modification with AgNPs, an Ag-O peak is also detected (516 cm^{-1}). The SEM-EDX analysis results indicate that Ag(20)/Zn-MOF has a cubic shape with 265-193 nm dimensions. Its form is heterogeneous, irregular, and rough, with AgNP aggregates measuring around 20-50 nm on the surface. TGA analysis results show that modifying AgNPs can enhance the thermal stability of Zn-MOF. Quantum chemical characteristics by the DFT method show that Ag/Zn-MOF is an excellent electron acceptor, which can increase the production of Reactive oxygen species (ROS), which can increase antibacterial properties.The antibacterial activity *(in vitro)* analysis data reveals that Ag(20)/Zn-MOF exhibits the highest inhibitory effect against ulcer-causing bacteria. In conclusion, this study demonstrates that Ag(20)/Zn-MOF is effective as an antibacterial material for diabetic ulcers.

KEYWORDS: Ag/Zn-MOF, Metal Organic Framework, DFT, Antibacterial, Ulcus Diabetic

INTRODUCTION :

Diabetes Mellitus (DM) is a group of metabolic diseases characterized by high blood sugar levels over a prolonged period. Elevated blood sugar levels can lead to symptoms such as frequent urination, increased thirst, and heightened hunger[1,2]. Diabetes can cause both acute and chronic complications[3]. The most common complications in diabetic patients are pathological changes in the extremities, including foot pain and the development of wounds [4,5]. In Indonesia, it is estimated that 17-32% of patients with DM die due to complications, and 15-30% of them undergo amputations as a result[6].

Complications of wounds in patients with diabetes, also known as diabetic ulcers, are usually characterized by pus-filled boils (PUS) caused by bacterial infections. The rapid growth of bacteria in diabetic wounds makes them difficult to heal. This is due to high blood sugar levels, which provide an ideal environment for bacterial development[7]. Research by Thanganadar[8] found that out of 50 samples from diabetic ulcer wounds, 85 isolates of both gram-positive and gram-negative bacteria were identified, with the majority being *Staphylococcus aureus* (38%), *Pseudomonas aeruginosa* (23.2%), *Bacillus subtilis* (21%), and *Escherichia coli* (18%). All the bacteria found were confirmed to be multi-antibiotic resistant at the wound site in diabetic patients. This result demonstrates the importance of developing new compounds that can be antibacterials for diabetic ulcers. One of the approaches being developed to address the issue of bacterial resistance in diabetic ulcers is the Metal-Organic Framework (MOF) development.

MOFs are porous materials composed of metal ions or metal clusters connected by various organic ligands to form a framework[9–11]. MOFs can oxidize and depolarize the outer cell membranes of bacteria, thereby inhibiting bacterial protein synthesis. One type of MOF developed as an antibacterial agent is Zinc (Zn)-MOF. Research by AbouAitah[12] has shown that MOF-74 and MOF-5 can inhibit the growth of *E. Coli* and *K. Pneumonia* bacteria from 80% to 99.9%. These results also demonstrate the potential of Zn-MOF in addressing bacterial resistance issues.

MOF also has other advantages, namely synergistic effects when modified with other compounds. Research by Bashar[13] shows that the modification of Zn-MOF with Fe_3O_4 results in a combination of properties from both compounds, namely nanoparticle properties and magnetic strength. Fe_3O_4/ZnMOF has been proven to have a specific surface area of 37,500 m^2/g and antibacterial activity against *Pseudomonas aeruginosa*, *shigella dysenteriae*, *Rhodococcus equi*, and *Streptococcus aphthae*, which is higher compared to conventional antimicrobial drugs. These results indicate significant potential for developing and modifying MOF as antibacterial materials[14,15].

Nanosilver (AgNPs) has been known for its antibacterial properties for a long time due to its broad antibacterial spectrum and lower drug resistance[16–18]. The modification of Ag in MOFs has also been proven to enhance effectiveness in inhibiting bacterial growth. Research by Shakya[19] showed that silver-modified Co-MOF (HKUST-1) reduced 90% of *Escherichia coli* and *Staphylococcus aureus* bacteria. Similar results were also demonstrated by Wu[20], who reported that Ag@MOF-5 could reduce 99% of *E. Coli* and *S. aureus* bacteria and have potential for development in the biomedical field.

In this study, Zn-MOF will be modified with silver nanoparticles and tested for antibacterial activity against both gram-positive and gram-negative bacteria. The bacteria used in this study are cultured from wound swabs of diabetes mellitus (DM) patients at "X" Hospital in Nganjuk. Additionally, the Gaussian application will perform computational stability and energy interaction studies of Ag/Zn-MOF using Density Functional Theory (DFT)[21–23].

MATERIALS AND METHODS:

Materials

The materials used are Zinc (II) nitrate hexahydrate ($Zn(NO_3)_2 \cdot 6H_2O$), silver nitrate ($AgNO_3$), and 1,4-benzene dicarboxylic acid (H_2BDC) with a purity of 99.0%, supplied by Sigma-Aldrich; N, N-dimethylformamide (DMF), chloroform ($CHCl_3$), methanol (CH_3OH), BAP (Blood Agar Plate), MSA (Manitol Salt Agar), NA (Nutrient Agar), MCA (Mac Conkey Agar), and Mueller-Hinton Agar (MHA) with a purity of 99.0%, supplied by Merck.

Method of Synthesis Zn-MOF

The synthesis of Zn-MOF was carried out by modifying the research of Ediati et al.[11] and Hu et al.[24]. $Zn(NO_3)_2 \cdot 6H_2O$ and H_2BDC (in a 3:1 mmol ratio) were initially reacted in 60 mL of DMF and stirred for 30 minutes. The solution was then placed in a closed reaction vessel and heated in an oven at 120°C for 24 hours under static conditions. The resulting solid was decanted and washed three times with DMF and three times with chloroform. The solid was then dried under vacuum at 60°C until completely dry and subsequently named Zn-MOF.

Method of modifying Zn-MOF with AgNPs

The modification method of Zn-MOF with silver nanoparticles (AgNPs) was carried out by modifying the research of Sacourbaravi et al.[25] and Hu et al.[24]. One gram of Zn-MOF was dissolved in chloroform and stirred for five days. The resulting solid was centrifuged and dried at 80°C for 24 hours. The obtained solid (0.1 gram) was dissolved in 10 mL of ethanol, and then AgNO3 (in ethanol) was slowly added at various concentrations (10 mg/mL and 20 mg/mL) using an ultrasonicator. The presence of Ag ions was measured using KCl. The resulting material at this stage is the modified MOF-5, referred to as Ag(10)/Zn-MOF and Ag(20)/Zn-MOF.

Characterization of Zn-MOF and Ag/Zn-MOF

The characterization of Zn-MOF and Ag/Zn-MOF materials was conducted using Powder X-ray diffraction (PXRD), Attenuated Total Reflectance Fourier Transform Infrared Spectroscopy (ATR FTIR), Scanning Electron Microscope, and Energy Dispersive X-ray Spectroscopy (SEM-EDX), as well as Thermogravimetric Analysis (TGA) and Differential Scanning Calorimetry (DSC). Functional group analysis was performed using ATR FTIR from Shimadzu Corporation, Japan, in the 400–4000 cm^{-1} wavenumber range. Difractogram pattern analysis was performed using XRD with a JEOL diffractometer using Cu Ka radiation (λ = 1.54056 Å) in the 5–50° range. Surface morphology and elemental composition were analyzed using SEM (Zeiss EVO MA10) with gold coating. Thermal stability analysis was performed using TGA (Mettler Toledo).

Analysis of structure and energy interactions through Density Functional Theory (DFT) study

The modified Zn-MOF molecule with AgNPs was optimized using Gaussian 09 version 6.0. The relative stability was determined by calculating the minimum energy of the modified Zn-MOF with AgNPs using the DFT/B3LYP method and LANL2DZ basis set in Gaussian09, as per the research by Moghadam et al.[26]. The DFT results were further utilized to determine its chemical properties through analysis of the Highest Occupied Molecular Orbital (HOMO) and Low Unoccupied Molecular Orbital (LUMO).

Identification of bacteria from diabetic ulcer patients

Identification of bacteria from diabetic ulcer patients was conducted according to the research by Khan et al. [27] and Bouharkat et al.[28]. The bacteria used in this study were cultured from wound specimens of diabetic patients at "X" Hospital in Nganjuk. In this stage, a modified procedure from Surya, dkk[29] was used, where diabetic ulcer specimens (PUS specimens) were collected using the swabbing method with sterile cotton swabs three times. These swabs were then placed in sterile tubes containing PZ. Gram-positive bacteria were identified by inoculating the specimen onto Blood Agar Plate (BAP) media, followed by incubation at 37°C for 24 hours. The results were observed through Gram staining under a microscope, including the shape, color, arrangement, and staining properties. Colonies from BAP media were subsequently inoculated onto Mannitol Salt Agar (MSA) and Nutrient Agar (NA) media and incubated at 37°C for 24 hours. The results were observed for shape, size, color, edge, surface, consistency, and pigmentation. Gram-negative bacteria are identified by inoculating the specimen onto Mac Conkey Agar (MCA) media, followed by incubation at 37°C for 24 hours. The results are then subjected to Gram staining and observed under a microscope, including their shape, color, arrangement, and staining properties.

Antibacterial activity of the causative agent of diabetic ulcers *in vitro*

All formed materials, namely Zn-MOF, Ag(10)/Zn-MOF, and Ag(20)/Zn-MOF, were subsequently tested for antibacterial activity related to diabetic ulcers in vitro by modifying the research of Sacourbaravi et al.[25] and Tian et al. (2022). Discs with a diameter of 6 mm were saturated in Zn-MOF, Ag(10)/Zn-MOF, and Ag(20)/Zn-MOF solutions at a concentration of 5 mg/mL for 30 minutes. The solid MHA medium, which had been sterilized, was then swabbed with bacteria isolated from diabetic ulcer samples. The saturated discs were placed on the MHA medium previously swabbed with the bacterial suspension from the ulcer culture. In this study, amoxicillin discs were used as a comparison. The MHA medium was incubated for 24 hours at 37°C in an incubator. The formation of clear inhibition zones indicated antibacterial activity, and the results were measured using a caliper.

RESULT:

Synthesis of Zn-MOF and Ag/Zn-MOF

Zn-MOF is produced by reacting $Zn(NO_3)_2•6H_2O$ metal and H_2BDC ligand in DMF solvent using the solvothermal method. The presence of a white solid indicates the formation of Zn-MOF. Zn-MOF is modified with AgNPs by reacting Zn-MOF with $AgNO_3$ in methanol solvent. The method used is sonication, utilizing ultrasonic waves. The formation of a green-brown solid indicates the successful synthesis of Ag(10)/Zn-MOF and Ag(20)/Zn-MOF. An illustration of the formation of Zn-MOF and Ag/Zn-MOF is shown in Figure 1.

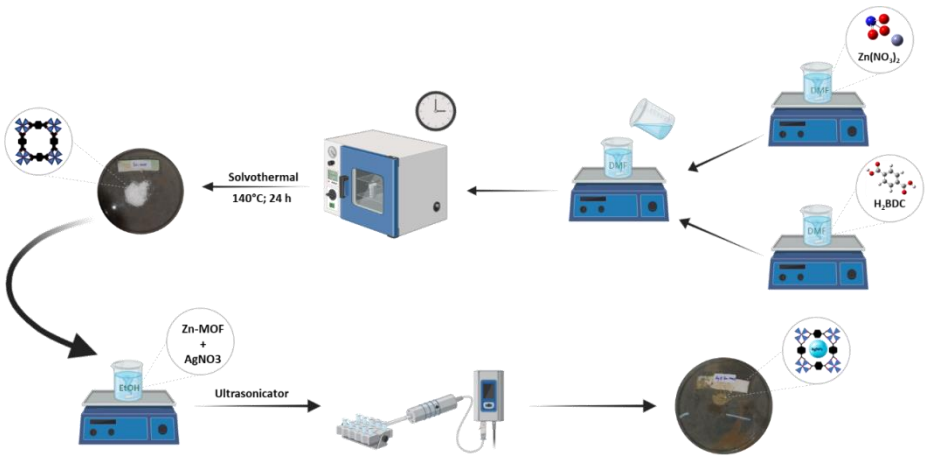

Figure 1. Illustration of the Zn-MOF and Ag/Zn-MOF Synthesis Process

Characterization of Zn-MOF and Ag/Zn-MOF

Analysis of PXRD

The comparison of diffraction patterns between Zn-MOF and Ag/Zn-MOF is shown in the figure 2.

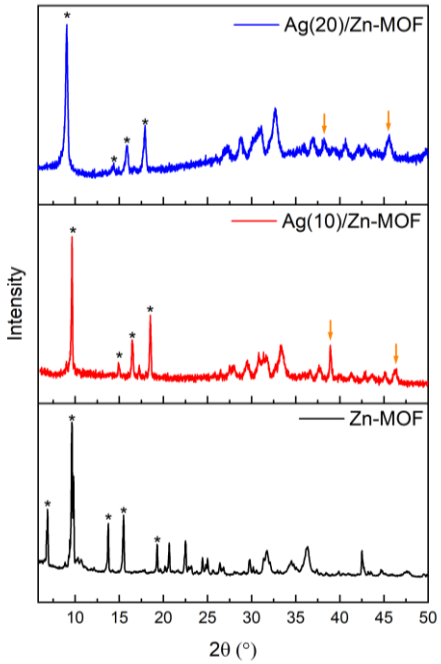

Figure 2. Difractogram Patterns of Zn-MOF and Ag/Zn-MOF

XRD analysis aims to determine the structure and phases of Zn-MOF and Ag/Zn-MOF. The PXRD results are also used to verify the successful modification of Zn-MOF with AgNPs through peak shifts, intensity changes, and the formation of new diffraction peaks. Figure 2 indicates that Zn-MOF exhibits characteristic peaks at 2θ = 6.8°, 9.6°, 13.7°, 15.5°, and 19.2°. After modification with AgNPs, there are changes in the diffraction pattern with the addition of several new peaks. Ag(10)/Zn-MOF shows characteristic peaks at 2θ = 9.6°, 14.9°, 16.4°, 18.5°, 38.8°, and 45.9°, while Ag(20)/Zn-MOF exhibits characteristic peaks at 2θ = 9.6°, 14.3°, 15.8°, 17.9°, 38.2°, and 45.6°. Subsequently, the characteristic peak values (2θ) of Zn-MOF and Ag-modified Zn-MOF are used to calculate microstrain and grain size using Scherrer's equation.

$$D = \frac{k\lambda}{\beta \cos\theta} \quad \text{and} \quad \varepsilon = \frac{\beta}{4 \tan\theta}$$

there are

D = average crystallite size

ε = microstrain

k = Scherrer constant (0,9)

λ = X-ray wavelength

β = FWHM (Full Width at Half Maximum)

θ = Bragg Angle

The average microstrain and grain size comparisons between Zn-MOF and Ag/ Zn-MOF are shown in figure 3. The respective average microstrains for Zn-MOF, Ag(10)/Zn-MOF, and Ag(20)/Zn-MOF are $7.82x10^{-3}$, $8.34x10^{-3}$, and $11.45x10^{-3}$, while the grain sizes for Zn-MOF, Ag(10)/Zn-MOF, and Ag(20)/Zn-MOF are 47.57 nm, 31.98 nm, and 22.56 nm, respectively.

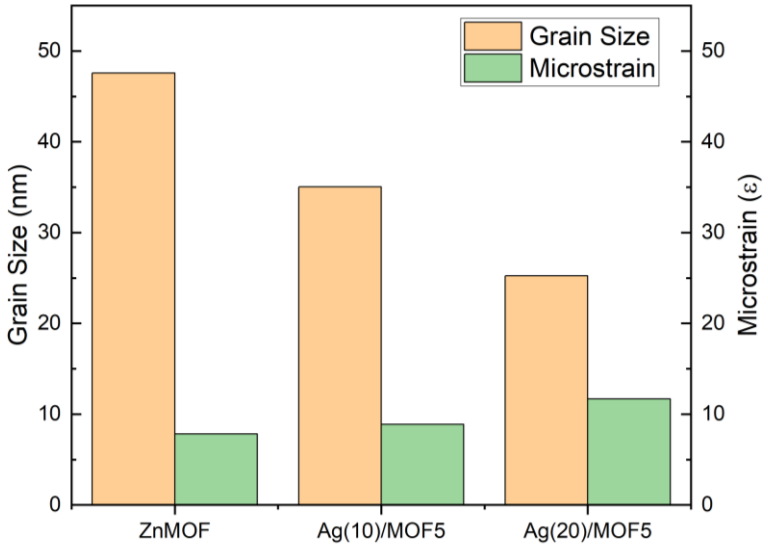

Figure 3. Comparison of microstrain and grain size of Zn-MOF and Ag/ Zn-MOF

Analysis of ATR-FTIR

The comparison of ATR-FTIR spectra between Zn-MOF and Ag/Zn-MOF is shown in Figure 4. ATR-FTIR analysis was conducted to identify the functional groups of Zn-MOF before and after AgNPs modification and to predict the success of Zn-MOF modification with AgNPs through shifts in wavenumber, intensity changes, and the formation of new absorption bands. Figure 4 indicates that Zn-MOF exhibits several absorption peaks at 3605 dan 3178 cm^{-1} (ν-OH), 1584 cm^{-1} (ν-COO_{assym}), 1547 dan 1501 cm^{-1} (νC=C), 1393 cm-1 (ν-COO_{sym}), 1014 cm-1 (νC-O) 1501 cm^{-1} (νC=C), 819 cm-1 (νC-C), 752 cm-1 (νC-H) serta 657 cm-1 (νZn-O). On the other hand, Ag(10)/Zn-MOF shows absorption peaks at 3603 and 3310 cm^{-1} (ν-OH), 1574 cm^{-1} (ν-COO_{assym}), 1499 cm^{-1} (νC=C), 1365 cm^{-1} (ν-COO_{sym}), 1014 cm^{-1} (νC-O), 808 cm^{-1} (νC-C), 744 cm^{-1} (νC-H), 647 cm^{-1} (νZn-O), and 518 cm^{-1} (νAg-O). In this study, the ATR-FTIR spectra of Ag(20)/Zn-MOF are similar to Ag(10)/Zn-MOF, both showing absorption peaks at 3602 and 3285 cm^{-1} (ν-OH), 1573 cm^{-1} (ν-COO_{assym}), 1499 cm^{-1} (νC=C), 1365 cm^{-1} (ν-COO_{sym}), 1014 cm^{-1} (νC-O), 807 cm^{-1} (νC-C), 743 cm^{-1} (νC-H), 646 cm^{-1} (νZn-O), and 516 cm^{-1} (νAg-O).

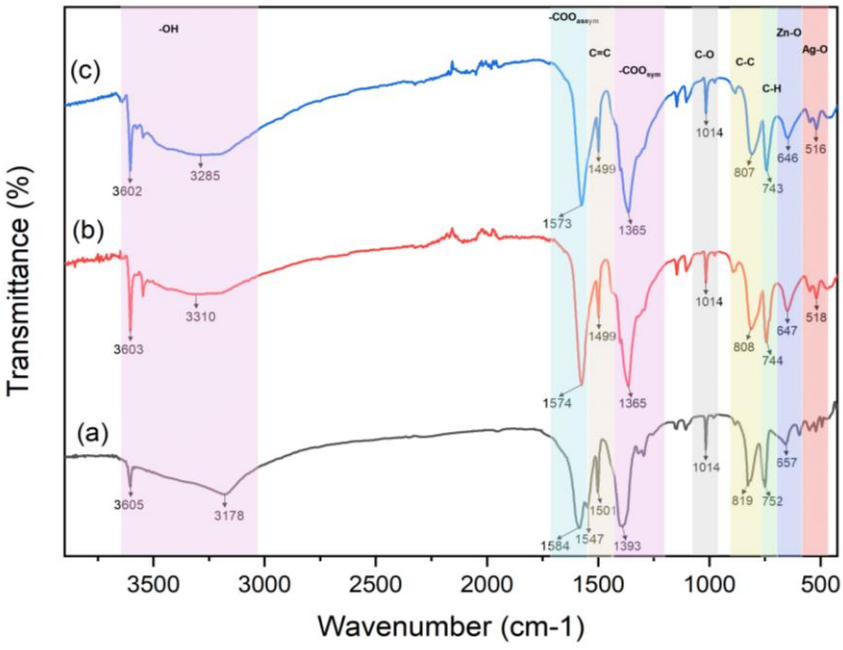

Figure 4. The ATR-FTIR Spectra of (a) Zn-MOF, (b) Ag(10)/Zn-MOF, and (c) Ag(20)/Zn-MOF

Analysis of SEM-EDX

The SEM-EDX analysis aims to examine the morphology and surface structure of Zn-MOF before and after AgNPs modification. In this study, SEM-EDX analysis was conducted on Zn-MOF and Ag(20)/Zn-MOF to measure the size and distribution of AgNPs on the Zn-MOF surface, as well as to identify the elements present in Zn-MOF and Ag(20)/Zn-MOF. SEM images of Zn-MOF and Ag(20)/Zn-MOF are shown in Figure 5. The composition of elements (wt%) in Zn-MOF and Ag(20)/Zn-MOF is shown in Table 1, while the distribution of elements in Ag(20)/Zn-MOF is shown in Figure 6.

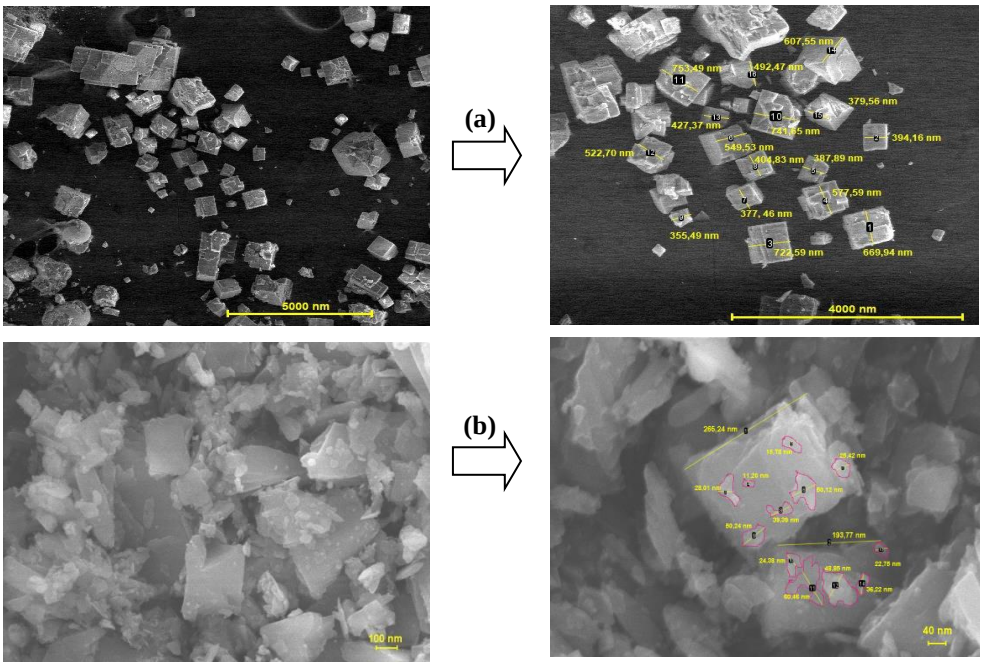

Figure 5. Analysis of Morphology of (a) Zn-MOF and (b) Ag(20)/Zn-MOF

Table 1. The Composition of Elements (wt%) for Zn-MOF and Ag(20)/Zn-MOF

Sample	Composition of Elements (wt%)			
	C	H	O	Ag
Zn-MOF	9.91±0.32	9.43±0.26	3.84±0.11	38.74±1.02
Ag(20)/Zn-MOF	9.62±0.23	9.21±0.21	5.63±0.16	58.52±1.06

Figure 5 reveals that Zn-MOF has a regular cubic morphology, whereas Ag(20)/Zn-MOF exhibits irregular morphology but still contains cubic-shaped solid particles with AgNPs distribution on the surface. The EDX analysis results confirm that Zn-MOF contains zinc (Zn) at 37.50 wt%, carbon (C) at 34.20 wt%, and oxygen (O) at 28.30 wt%, while Ag(20)/Zn-MOF includes zinc (Zn) at 54.27 wt%, carbon (C) at 23.81%, oxygen (O) at 20.77 wt%, and silver (Ag) at 1.15%.

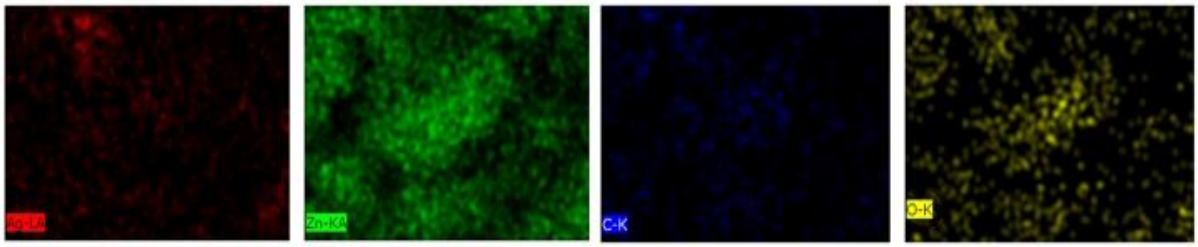

Figure 6. The Distribution of Elements in Ag(20)/Zn-MOF

Analysis of TGA

The TGA analysis was conducted to determine the thermal stability of Zn-MOF before and after AgNPs modification. In this study, the impact of AgNP modification on the thermal stability of Zn-MOF was assessed by comparing the TGA results of Zn-MOF and Ag(20)/Zn-MOF. Figure 7 shows that Zn-MOF undergoes degradation at low temperatures up to 180°C, with a weight loss percentage of 22 wt%, and experiences main decomposition between 420°C and 550°C, with a weight loss percentage of 60 wt%. The Ag(20)/Zn-MOF material undergoes degradation between 420°C and 480°C, with a weight loss percentage of 50 wt%.

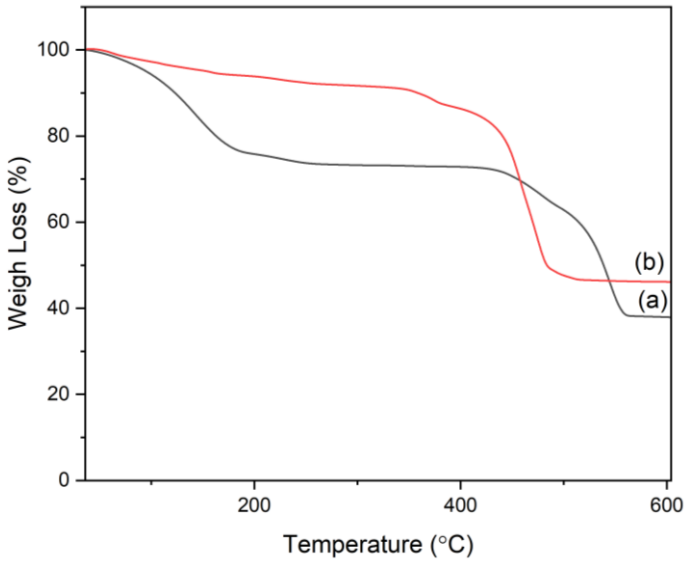

Figure 7. The TGA Result (a) Zn-MOF (b) Ag(20)/Zn-MOF

Analysis of structure and energy interactions through Density Functional Theory (DFT) study

Computational analysis using the DFT (Density Functional Theory) method was carried out to design and optimize Zn-MOF and Ag/Zn-MOF compounds for a broader range of applications. In this study, a LANL2DZ set base was used. The optimized structure of Zn-MOF and Ag/Zn-MOF by the DFT method is shown in Figure 8. Figure 8 shows that Zn-MOF originally had a binding energy of -732.248 Kcal/mol and Ag/Zn-MOF of -877.177 kcal/mol. AgNPs-modified Zn-MOF have a physical bond between Zn_{14} and Ag with a bond length of 2.705 Å and do not significantly change the bond length of the individual Zn-MOF structures.

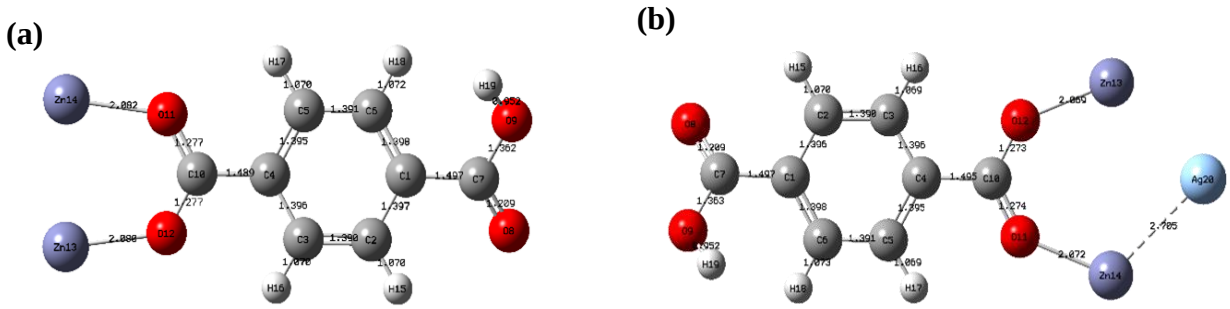

Figure 8. The results of compound optimization using DFT with a set base of LANL2DZ: (a) Zn-MOF and (b) Ag/Zn-MOF

The results of DFT analysis are then used for HOMO-LUMO analysis to determine the chemical properties of Zn-MOF and Ag/Zn-MOF. The results of the HOMO-LUMO analysis for the material are shown in Figure 9. The results of the quantum chemical descriptor show the chemical characteristics of the material, such as chemical potential (μ), chemical hardness (η), softness (S), electronegativity (χ) and electrophilicity (ω), as shown in Table 2.

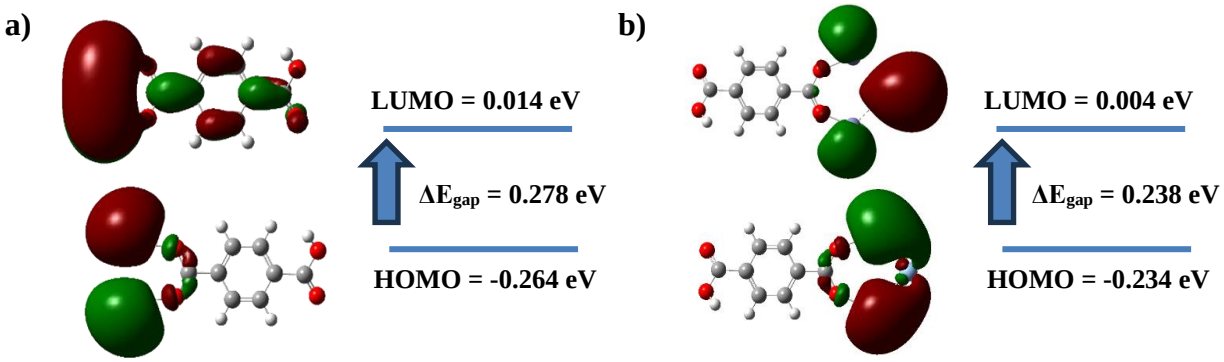

Figure 9. HOMO-LUMO surface of: a) Zn-MOF and b) Ag/Zn-MOF

Figure 9 shows that HOMO in Zn-MOF electrons is delocalized, especially in the central metal, namely Zn, while in Ag/Zn-MOF electrons are delocalized in the central metal, Zn and Ag metal. LUMO in Zn-MOF shows electrons delocalized in the benzene ring of the ligand, whereas in Ag/Zn-MOF, electrons are delocalized in the central metal Zn and Ag metal.

Table 2. Quantum chemistry descriptor for Zn-MOF and Ag/Zn-MOF

Sample	E_{LUMO} (eV)	E_{HOMO} (eV)	ΔE_{gap} (eV)	μ (eV)	η (eV)	S (eV)	χ (eV)	ω (eV)
Zn-MOF	0,014	-0,264	0,278	-0,125	0,139	0,0695	0,125	0,056
Ag/Zn-MOF	0,004	-0,234	0,238	-0,115	0,119	0,0595	0,115	0,056

Table 2 shows that the energy gap value of Zn-MOF after modification with Ag (Ag/Zn-MOF) is smaller (0.234 eV) compared to individual Zn-MOF (0.278 eV). The chemical hardness and chemical potential values of Ag/Zn-MOF are 0.119 eV and -0.125, respectively, while Zn-MOF is 0.139 eV and -0.115 eV

Identification of bacteria from diabetic ulcer patients

Pus samples from diabetic ulcer patients were found to contain 1 type of gram-positive bacteria, that is *Staphylococcus aureus*, and 3 types of gram-negative bacteria, *Escherichia coli*, *Pseudomonas aeruginosa*, and *Klebsiella spp*. These results were obtained from several biochemical characteristics and bacterial staining tests shown in Table 3.

Table 3. The Biochemical Characteristics and Bacterial Staining Tests From Ulcer Patients

Test	*Staphylococcus aureus*	Escheria coli	*Pseudomonas aeruginosa*	*Klebsiella spp*
Gram'stain	+	-	-	-
Motility	NM	M	M	M
Oksidase	-	-	+	-
Citrate	+	-	+	+
Urease	+	+	+	+
Catalase	+	-	-	+
TSI	Acid/Acid	Acid/Acid	Alkali/Alkali	Acid/Acid
Indole Production	-	+	-	-
Methyle red	+	+	-	-
Glucose fermentation	+	+	-	+
Lactose fermentation	+	+	-	+
Staining	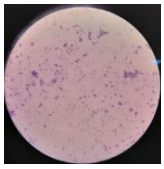	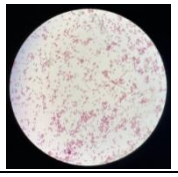	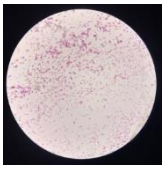	
Morphology	coccus	basil	basil	basil

Test for antibacterial activity of diabetic ulcer causes in vitro

The results of the antibacterial activity test on Zn-MOF and Ag/Zn-MOF are shown through the clear inhibition zone around the disc (Figure 10). In this study, the antibacterial activity of the cause of diabetic ulcers was also tested on amoxilin antibiotics as a comparison. Comparison of the results of the antibacterial activity test for diabetic ulcers on Zn-MOF, Ag(10)/Zn-MOF, Ag(20)/Zn-MOF, amoxilin, and several other active substances is shown in Table 3.

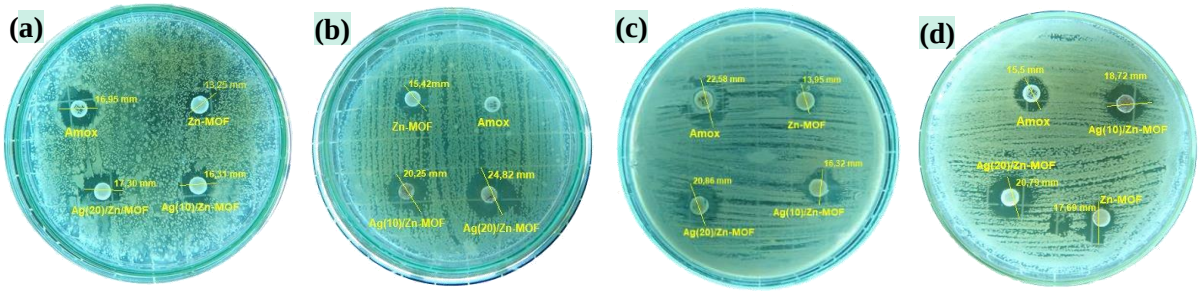

Figure 10. The results of the antibacterial activity test on Zn-MOF and AgNPs modified Zn-MOF (a) *Staphylococcus aureus* (b) Escheria coli (c) *Pseudomonas aeruginosa* (d) *Klebsiella spp*

Table 3 shows that Ag(20)/Zn-MOF has the greatest inhibition against bacteria that cause diabetic ulcers, namely 24.82 mm against *Escherichia coli*, 20.86 mm against *Pseudomonas aeruginosa*, 20.79 mm against *Klebsiella spp* and 17.30 mm against *Staphylococcus aureus*. When compared with other active substances, both plant extracts and other types of MOF, Ag/Zn-MOF has high inhibition against bacteria that cause ulcers.

Table 3. The Results of The Antibacterial Activity Test for Diabetic Ulcers

Sample	Concentration (mg/mL)	Zone of inhibition (mm)				Ref
		Staphylococcus aureus	Escheria coli	*Pseudomonas aeruginosa*	*Klebsiella spp*	
Zn-MOF	2	13,25	15,42	13,95	17,69	This work
Ag(10)/Zn-MOF	2	16,31	20,25	16,32	18,72	This work
Ag(20)/Zn-MOF	2	17,30	24,82	20,86	20,79	This work
Amoxilin	250	16,95	0	22,58	15,5	This work
A.marmelos	100	12,2	9,1	15,1	-	[30]
T.involucurata	20	3,4	2,5	3,4	1,2	[31]
S.Auriculata (L)	80	11,66	9,66	11	-	[32]
Zn-MOF$_{(pyridine)}$	2	17	8,6	-	9,7	[33]
Cu/DPA-MOF	10	18,43	16,61	-	17,04	[34]
Ag/UiO-66-NH$_2$	35	9,01	7,45	-	-	[35]

DISCUSSION:

In this study, the formation of white solids shows the success of Zn/MOF synthesis. This result is similar to the research of Ediati et al[11], which showed the presence of white crystals as an indicator of the formation of Zn-MOF. The synthesis of Ag nano-modified Zn-MOF is carried out by sonication method because ultrasonic waves can evenly disperse Ag metals in the MOF and direct the rapid formation of MOF nanoparticles at room temperature and atmospheric pressure[25,36]. The success of Ag/Zn-MOF synthesis is shown through the formation of brownish-green solids. This result is similar to the research of Hu et al.[24], which shows that modification of Zn-MOF with AgNPs will produce dark green crystals. The discolouration of the nano-modified Zn-MOF is an early indication of an interaction between AgNPs and the Zn-MOF. This result is similar to Pereira et al.'s[37] research, which reported that the initial indication of MOF-74 decoration with Au and Ag nanoparticles is the discolouration seen in the crystals. This is due to several things, such as the Plasmonic Effect of Nano Au and Ag, which causes an increase in the absorption and spread of light and the distribution of Nano Au and Ag on the surface of MOF-74 so that it affects the optical properties of the material.

Zn-MOF has a diffractogram pattern with characteristic peaks, according to the research of Ediati et al.[11] and Hu et al.[24]. These results show that Zn-MOF has been successfully synthesized. The results of XRD analysis show that Ag(10)/Zn-MOF and Ag(20)/Zn-MOF have a diffractogram pattern similar to Zn-MOF, but there are some shifts and the addition of new peaks. The peak of Zn-MOF characteristics at 2θ = 9.6º is still visible in the Difrectogram patterns Ag(10)/Zn-MOF and Ag(20)/Zn-MOF with high intensity. This shows that the structure of Zn-MOF has not changed or is stable[35]. On the other hand, some peaks of Zn-MOF characteristics have shifted after the modification of the AgNPs, indicating the AgNP modification's success. This result is strengthened by the presence of new peaks at Ag(10)/Zn-MOF at 2θ = 38.8º and 45.9º and new peaks at Ag(20)/Zn-MOF at 2θ = 38.2º and 45.6º which show typical fields (111) and (200) as characteristic peaks of Ag_2O and AgO[25]. This result is similar to the research of MaO et al.[38], which showed that at CubpyCl/0.25Ag, the characteristic peaks of Cu-MOF still consistently appeared. However, there were also small peaks in the region of 2θ = 38.1º caused by the presence of AgNPs on the surface of Cu-MOF. The peak intensity of Ag characteristics at Ag(10)/Zn-MOF and Ag(20)/Zn-MOF at the peaks of the regions 2θ = 38º and 45º may be due to the difference in the number of Ag nanos interacting with Zn-MOF. The peak characteristic of Zn-MOF and Ag/Zn-MOF was then used to calculate the microstrain value and grain size. The calculation results of the average microstrain and grain size show that the greater the AgNP concentration, the microstrain will increase, and the grain size will decrease. This is due to the presence of AgNPs on the surface of Zn-MOF, causing deformation of the Zn-MOF lattice, which causes crystal defects so that microstrains increase. In addition, the existence of AgNPs with a tiny size also causes the grain size of Ag(20)/Zn-MOF to be smaller when compared to others[39].

The success of Zn-MOF synthesis is shown from several characteristic functional group vibrations that appear on the ATR-FTIR spectra, such as O-H vibration that shows water vapour on the surface of Zn-MOF [24,35,40] and the presence of -COO_{sym} and –COO_{asym} vibrations that indicate a bond between the carboxyl group of the ligand and the central metal Zn[24]. This is strengthened by the presence of Zn-O vibration in the fingerprint area, indicating a Zn_4O metal cluster[41]. Other absorption bands that support the confirmation of the formation of Zn-MOF include C-C and C-O vibrations from benzene ligands dicarboxylates and C=C and C-H from benzene rings [42]. Modification of Zn-MOF with AgNPs is confirmed by the shift of -COO_{sym} and –COO_{asym} vibrations to lower wave numbers due to the interaction of carbonyl groups with AgNPs[24]. This result is strengthened by a new peak in the fingerprint area, indicating AgO vibration[43]. The shift in the C=C and C-H absorption bands indicates the deformation of the benzene group in the ligan. This result is consistent with the XRD analysis, which shows that the modification of Zn-MOF with AgNPs has been successfully carried out.

The results of SEM-EDX analysis show that Zn-MOF has an irregular cubic shape with a size varying from 355 nm to 753 nm while Ag(20)/Zn-MOF has a cubic shape with a size of 265-193 nm, but the shape is heterogeneous, irregular, and rougher. This result is consistent with XRD analysis, which shows that Ag(20)/Zn-

MOF has a larger microstrain and indicates the presence of crystal defects. In addition, on the surface of Ag(20)/Zn-MOF, AgNPs are scattered on the surface with sizes varying from 11-60 nm. This result is also supported by EDX data, which shows the presence of AgNPs as an additional Ag(20)/Zn-MOF forming element. This is to the research of Hootifard et al.[39], who reported that Co-MOF@Ag2O has a heterogeneous surface structure and the presence of AgNPs aggregated on the surface of Co-MOF with sizes varying from 11-30 nm. The results of the TGA analysis showed that Zn-MOF degraded at low temperatures due to the release of water vapour and residual DMF solvents. In contrast, the primary degradation of Zn-MOF at high temperatures was caused by the release of organic groups and the decomposition of the Zn-MOF skeleton[44]. The results of the TGA Ag(20)/Zn-MOF analysis show that degradation only occurs at high temperatures because AgNPs can strengthen the coordination bond with the benzene dicarboxylate ligand so that Ag(20)/Zn-MOF tends to be more stable and has better thermal stability[24,39,45]. The mass of Ag(20)/Zn-MOF residue is higher than that of Zn-MOF due to the interaction of AgNPs in Zn-MOF[46]. These results also verify that modifying with AgNPs can improve the thermal stability of Zn-MOF.

The results of structural optimization with DFT showed that there was an energy change after modification with AgNPs. This indicates an increase in the reactivity of Zn-MOF so that the modification of AgNPs in Zn-MOF can increase its effectiveness[47]. In addition, the DFT results showed no change in the chemical structure of Zn-MOF after the modification of AgNPs, so it did not change the physicochemical properties of Zn-MOF, especially as an antibacterial[48]. The results of the HOMO-LUMO calculation highlight that the presence of a second metal ion, such as Ag, can significantly alter the pattern of electronic delocalization in MOFs, leading to more complex and potentially stable or functional materials[49]. Modification of Zn-MOF with Ag can also lead to a reduction in HOMO and LUMO energies as well as a narrower HOMO-LUMO energy gap due to electronic interactions, structural changes, and functionalization effects[47]. HOMO-LUMO results also show a lower energy gap, indicating that the electron density can be changed more efficiently, thus making the molecule more polarized and reactive[50]. These results are supported by chemical hardness values that show increased reactivity and chemical potential values that show the stability of Ag/Zn-MOF structures[51]. Quantum chemical characteristics data explain that the addition of AgNPs to Zn-MOF increases the ability of electron acceptors to be excellent so that it can increase the production of Reactive oxygen species (ROS), which can increase the antibacterial properties of Ag/Zn-MOF[52].

The results of bacterial identification in pus samples from Diabetes Mellitus (DM) patients showed that 4 types of bacteria were found, namely *Staphylococcus aureus*, *Escherichia coli*, *Pseudomonas aeruginosa*, and *Klebsiella spp*. Several types of bacteria can be found in diabetic ulcer patients because ulcer wounds generally contain high sugar levels, making them suitable as a medium for bacterial growth. The presence of *Staphylococcus aureus*, *Escherichia coli*, and *Klebsiella spp* in diabetic ulcers is due to the presence of endogenous sources so that if DM patients have open wounds, *Staphylococcus aureus*, *Escherichia coli* and *Klebsiella spp* can colonize and infect diabetic ulcer wounds[53,54]. In addition, *Staphylococcus aureus* and *Pseudomonas aeruginosa* can form more resistant biofilms and can infect diabetic ulcer wounds. These results are by the research of Barrigah-Benissan et al.[55] and Stańkowska et al[56] who reported that the most common bacterial isolates found in the wounds of DM patients were *Staphylococcus aureus* and *Pseudomonas aeruginosa*. The results showed that Ag(20)/Zn-MOF had a higher antibacterial activity that causes diabetic ulcers when compared to Zn-MOF, amoxicillin, and other plant-active substances that have been reported. An illustration of the mechanism of Ag(20)/Zn-MOF as an antibacterial that causes diabetic ulcers is shown in Figure 11.

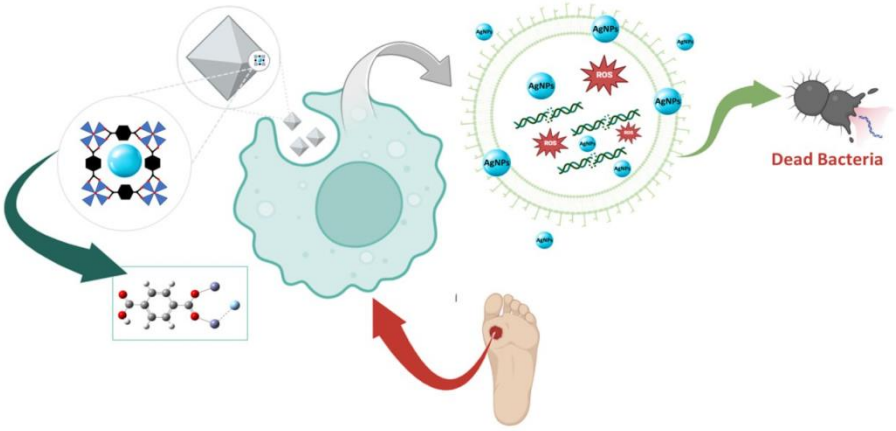

Figure 11.The Illustration of Mechanism Ag(20)/Zn-MOF as an Antibacterial that Causes Diabetic Ulcers

Ag(20)/Zn-MOF can inhibit the growth of bacteria, including bacteria that cause diabetic ulcers, because MOFs have a pore structure that can adsorb and depolarize bacterial membranes [57,58]. The release of the Zn centre metal can also lead to the formation of ROS (Reactive Oxygen Species), which can damage bacterial membranes and DNA[59]. The presence of AgNPs in Zn-MOF causes a synergistic effect, so the ability of Ag(20)/Zn-MOF to damage cell membranes and bacterial DNA increases. This causes the bacterial inhibition zone to increase. In addition, although the concentration of Ag(20)/Zn-MOF used to test the antibacterial activity that causes diabetic ulcers is small, the inhibitory zonat produced is the largest compared to others. Research Akbarzadeh[18] reports that MOFs have the advantage of long persistence, so even though the dose is low, the antibacterial activity is higher than that of antibiotics. These results show the effectiveness of Ag(20)/Zn-MOF as an antibacterial material that causes diabetic ulcers.

CONCLUSION:

The results of Zn-MOF synthesis by the solvothermal method produced white crystals, while Zn-MOF modified with AgNPs by the ultrasonication method obtained brownish-green solids from Ag/Zn-MOF. The results of XRD analysis show that Ag(10)/Zn-MOF and Ag(20)/Zn-MOF have a diffractogram pattern similar to Zn-MOF, but there are some shifts and the addition of new peaks in Ag(10)/Zn-MOF which are typical as characteristic peaks of Ag2O and AgO. The results of FTIR analysis The success of Zn-MOF synthesis showed the bond between the carboxylate group of the ligand and the central metal Zn and the presence of Zn-O vibration in the fingerprint region, indicating the presence of a Zn4O metal cluster. After modification with AgNPs, it was found that there was an Ag-O peak (516 cm-1). The results of the SEM-EDX analysis show that Zn-MOF has a regular cubic shape while Ag(20)/Zn-MOF has a heterogeneous, irregular, and coarser shape, with AgNP aggregates on the surface. The results of the TGA analysis showed that Ag nano modification can improve the thermal stability of Zn-MOF. The results of the DFT study show that Ag/Zn-MOF is an excellent electron acceptor, which can increase the production of reactive oxygen species (ROS) and increase antibacterial properties. The results of the antibacterial analysis showed that Ag(20)/Zn-MOF had the most significant inhibitory power against the bacteria that cause diabetic ulcers, namely 24.82 mm against *Escherichia coli* bacteria, 20.86 mm against *Pseudomonas aeruginosa*, 20.79 mm against *Klebsiella spp* bacteria and 17.30 mm against *Staphylococcus aureus* bacteria. Compared to other active substances, both plant extracts and other types of MOF, Ag(20)/Zn-MOF has the highest inhibitory power against ulcer-causing bacteria.

CONFLICT OF INTEREST:

The authors declare that they have no conflict of interest regarding this investigation.

ACKNOWLEDGMENTS:

The author expressed his gratitude to the DRTPM of the Republic of Indonesia for providing research funds through the Domestic Cooperation Research Grant (PKDN). The author also thanked the Institut Ilmu Kesehatan Bhakti Wiyata and Airlangga University for supporting the research process.

REFERENCES:

1. Kumar R, Saha P, Kumar Y, Sahana S, Dubey A, Prakash O. A review on diabetes mellitus: type1 & Type2. World J Pharm Pharm Sci. 2020;9:838–50.
2. Chaudhari A. A study to assess the knowledge regarding foot care among diabetes mellitus patients in selected hospital mehsana. Asian Journal of Nursing Education and Research. 2020;10:330.
3. Panari H, Vegunarani M. Study on Complications of Diabetes Mellitus among the Diabetic Patients. Asian Journal of Nursing Education and Research. 2016;6:171.
4. Logeshwary M, Somasundaram I. Quality of Life and Increasing Role of Biomarkers in Diagnosis, Prognosis and Prediction of Diabetic Foot Ulcer. Res J Pharm Technol. 2020;13:1597.
5. Logeshwary M, Somasundaram I. Effect of Bodyweight, Malnutrition and Lifestyle Modification on health related quality of life in Diabetic Foot Ulcer patients. Res J Pharm Technol. 2020;13:106.
6. Ardila N, Maharani R, Sabella A, Negara CK. The Effect of Wound Treatment Using Honey on Colonization of Staphylococcus Aureus Bacteria in Diabetic Wounds in Patients with Diabetes Mellitus in the Work Area Banjarmasin Health Center. 2022;
7. Albarrak OS. Wound Care Management Options for Diabetic Foot Ulcer. Saudi J Nurs Health Care. 2023;6:438–42.
8. Thanganadar Appapalam S, Muniyan A, Vasanthi Mohan K, Panchamoorthy R. A Study on Isolation, Characterization, and Exploration of Multiantibiotic-Resistant Bacteria in the Wound Site of Diabetic Foot Ulcer Patients. Int J Low Extrem Wounds [Internet]. 2019;20:6–14. Available from: https://doi.org/10.1177/1534734619884430
9. Pujiono FE, Mulyati TA. Synthesis and Characterization of UiO-66 as a Paracetamol Absorption Material. Al-Kimia. 2019;7:189–97.
10. Mansour O, Kawas G, Rasheed MA, Sakur AA. Applications of Metal-Organic Frameworks (MOFs) to Separation Analytical Techniques. Res J Pharm Technol. 2018;11:3514.
11. Ediati R, Mulyati TA, Mukminin A, Sulistiono DO, Khoiroh N, Fansuri H, et al. Nanoporous Carbon Prepared with MOF-5 as a Template and Activated using KOH for Hydrogen Storage. Jurnal Kimia Valensi [Internet]. 2020;6:20–31. Available from: https://doi.org/10.15408/jkv.v6i1.13621

12. AbouAitah K, Higazy IM, Swiderska-Sroda A, Abdelhameed RM, Gierlotka S, Mohamed TA, et al. Anti-inflammatory and antioxidant effects of nanoformulations composed of metal-organic frameworks delivering rutin and/or piperine natural agents. Drug Deliv. 2021;28:1478–95.
13. Bashar BS, Kareem HA, Hasan YM, Ahmad N, Alshehri AM, Al-Majdi K, et al. Application of novel Fe3O4/Zn-metal organic framework magnetic nanostructures as an antimicrobial agent and magnetic nanocatalyst in the synthesis of heterocyclic compounds. Front Chem. 2022;10:1014731.
14. Li R, Chen T, Pan X. Metal–organic-framework-based materials for antimicrobial applications. ACS Nano. 2021;15:3808–48.
15. Shen M, Forghani F, Kong X, Liu D, Ye X, Chen S, et al. Antibacterial applications of metal–organic frameworks and their composites. Compr Rev Food Sci Food Saf. 2020;19:1397–419.
16. Gaurav I, Tanuja. Green synthesis and characterization of silver nanoparticles with Rhizome extract of Curcuma longa (AgNPs-RECL) for Antimicrobial activity towards Xanthomonas and Erwinia species. Res J Pharm Technol. 2021;14:325–30.
17. Asha MA, Senthilkumar RS. Green synthesis and characterization of silver nanoparticles from Ocimum basilicum and their antimicrobial antioxidant and anticancer activity. Res J Pharm Technol. 2020;13:5711–5.
18. Akbarzadeh F, Motaghi M, Chauhan NPS, Sargazi G. A novel synthesis of new antibacterial nanostructures based on Zn-MOF compound: design, characterization and a high performance application. Heliyon. 2020;6:e03231.
19. Shakya S, He Y, Ren X, Guo T, Maharjan A, Luo T, et al. Ultrafine silver nanoparticles embedded in cyclodextrin metal-organic frameworks with GRGDS functionalization to promote antibacterial and wound healing application. Small. 2019;15:1901065.
20. Wu YM, Zhao PC, Jia B, Li Z, Yuan S, Li CH. A silver-functionalized metal–organic framework with effective antibacterial activity. New Journal of Chemistry. 2022;46:5922–6.
21. Adole VA, Bukane AR, Waghchaure RH, Shinde RS, Jagdale BS. Computational Study on Molecular Structure, UV-Visible and Vibrational Spectra and Frontier Molecular Orbital Analysis of (E)-7-((2-Chloroquinolin-3-yl)methylene)-1,2,6,7-tetrahydro-8H-indeno[5,4-b]furan-8-one. Res J Pharm Technol. 2022;1101–8.
22. Pawar RR, Nahire SB. Investigation, correlation and DFT study for solubility of malonic acid in water + methanol and water + ethanol binary solvents at T = 293.15 to 313.15 K. Res J Pharm Technol. 2021;14:1226–32.
23. Ghammamy S, Qaitmas NA, Lashgari A. Structural Properties, Natural Bond Orbital, Theory Functional Calculations (DFT), and Energies for the Two New Halo Organic Compounds. Asian Journal of Research in Chemistry. 2015;8:60.
24. Hu Y, Yang H, Wang R, Duan M. Fabricating Ag@MOF-5 nanoplates by the template of MOF-5 and evaluating its antibacterial activity. Colloids Surf A Physicochem Eng Asp [Internet]. 2021;626:127093. Available from: https://doi.org/10.1016/j.colsurfa.2021.127093
25. Sacourbaravi R, Ansari-Asl Z, Kooti M, Nobakht V, Darabpour E. Fabrication of Ag NPs/Zn-MOF Nanocomposites and Their Application as Antibacterial Agents. J Inorg Organomet Polym Mater [Internet]. 2020;30:4615–21. Available from: https://doi.org/10.1007/s10904-020-01601-x
26. Moghadam G, Abdi J, Banisharif F, Khataee A, Kosari M. Nanoarchitecturing hybridized metal-organic framework/graphene nanosheet for removal of an organic pollutant. J Mol Liq [Internet]. 2021;341:117323. Available from: https://doi.org/10.1016/j.molliq.2021.117323
27. Khan MS, Azam M, Khan MN, Syed F, Ali SHB, Malik TA, et al. Identification of contributing factors, microorganisms and antimicrobial resistance involved in the complication of diabetic foot ulcer treatment. Microb Pathog [Internet]. 2023;184:106363. Available from: https://doi.org/10.1016/j.micpath.2023.106363
28. Bouharkat B, Tir Touil A, Mullié C, Chelli N, Meddah B. Bacterial ecology and antibiotic resistance mechanisms of isolated resistant strains from diabetic foot infections in the north west of Algeria. J Diabetes Metab Disord. 2020;19:1261–71.
29. Surya SP, Dewi KP, Regina R. Cutaneous candidiasis mimicking inverse psoriasis lesion in a type 2 diabetes mellitus patient. Journal of General-Procedural Dermatology & Venereology Indonesia. 2020;5:7.
30. Hussain MSB, Hiremath MB. IN VITRO EVALUATION OF AEGLE MARMELOS LEAF EXTRACTS ON FOOT ULCER AND URINARY TRACT INFECTED PATHOGENS FROM DIABETIC PATIENTS. AsianJournalofPharmaceuticalandClinicalResearch. 2020;13:229–33.
31. Subbu Lakshmi S, Chelladurai G, Suresh B. In vitro studies on medicinal plants used against bacterial diabetic foot ulcer (BDFU) and urinary tract infected (UTI) causing pathogens. Journal of Parasitic Diseases. 2016;40:667–73.
32. Prasathkumar M, Raja K, Vasanth K, Khusro A, Sadhasivam S, Sahibzada MUK, et al. Phytochemical screening and in vitro antibacterial, antioxidant, anti-inflammatory, anti-diabetic, and wound healing attributes of Senna auriculata (L.) Roxb. leaves. Arabian Journal of Chemistry. 2021;14:103345.
33. Akbarzadeh F, Motaghi M, Chauhan NPS, Sargazi G. A novel synthesis of new antibacterial nanostructures based on Zn-MOF compound: design, characterization and a high performance application. Heliyon. 2020;6.
34. Jasim Al-Khafaji HH, Alsalamy A, Abed Jawad M, Ali Nasser H, Dawood AH, Hasan SY, et al. Synthesis of a novel Cu/DPA-MOF/OP/CS hydrogel with high capability in antimicrobial studies. Front Chem [Internet]. 2023;11. Available from: https://doi.org/10.3389/fchem.2023.1236580
35. Tian F, Weng R, Huang X, Chen G, Huang Z. Fabrication of Silver-Doped UiO-66-NH2 and Characterization of Antibacterial Materials. Coatings. 2022;12:1939.
36. Arul P, Gowthaman NSK, John SA, Lim HN. Ultrasonic Assisted Synthesis of Size-Controlled Cu-Metal–Organic Framework Decorated Graphene Oxide Composite: Sustainable Electrocatalyst for the Trace-Level Determination of Nitrite in Environmental Water Samples. ACS Omega [Internet]. 2020;5:14242–53. Available from: https://doi.org/10.1021/acsomega.9b03829
37. Pereira de Figueiredo JA, Moreno Zapata MJ, Amorim LS, de Oliveira Neto JA, Miquita DR, Soares EA, et al. Morphological and Structural Characterization of (Pt, Au, and Ag) Nanoparticle/Zn-MOF-74 Composites. ACS Omega [Internet]. 2024;9:21939–47. Available from: https://doi.org/10.1021/acsomega.3c09973
38. Mao F, Su Y, Sun X, Li B, Liu PF. Cu(I) Metal–Organic Framework Composites with AgCl/Ag Nanoparticles for Irradiation-Enhanced Antibacterial Activity against *E. coli*. ACS Omega [Internet]. 2023;8:2733–9. Available from: https://doi.org/10.1021/acsomega.2c07415
39. Hootifard G, Sheikhhosseini E, Ahmadi SA, Yahyazadehfar M. Synthesis and characterization of CO-MOF@ Ag2O nanocomposite and its application as a nano-organic catalyst for one-pot synthesis of pyrazolopyranopyrimidines. Sci Rep. 2023;13:17500.
40. Dahlan I, Keat OH, Aziz HA, Hung YT. Synthesis and characterization of MOF-5 incorporated waste-derived siliceous materials for the removal of malachite green dye from aqueous solution. Sustain Chem Pharm. 2023;31:100954.
41. Gyanendra K, Dhanraj TM. Sustainable synthesis of MOF-5@ GO nanocomposites for efficient removal of rhodamine B from water. ACS omega. 6, 14 (2021) 9587-9599.

42. Villarroel-Rocha D, Bernini MC, Arroyo-Gómez JJ, Villarroel-Rocha J, Sapag K. Synthesis of MOF-5 using terephthalic acid as a ligand obtained from polyethylene terephthalate (PET) waste and its test in CO2 adsorption. Brazilian Journal of Chemical Engineering. 2022;39:949–59.
43. Cai M, Qin L, You L, Yao Y, Wu H, Zhang Z, et al. Functionalization of MOF-5 with mono-substituents: effects on drug delivery behavior. RSC Adv. 2020;10:36862–72.
44. Zhou D, Wang L, Chen X, Wei X, Liang J, Tang R, et al. Reaction mechanism investigation on the esterification of rosin with glycerol over annealed Fe3O4/MOF-5 via kinetics and TGA-FTIR analysis. Chemical Engineering Journal. 2020;401:126024.
45. Kasula M, Le T, Thomsen A, Rabbani Esfahani M. Silver metal organic frameworks and copper metal organic frameworks immobilized on graphene oxide for enhanced adsorption in water treatment. Chemical Engineering Journal [Internet]. 2022;439:135542. Available from: https://doi.org/10.1016/j.cej.2022.135542
46. Hootifard G, Sheikhhosseini E, Ahmadi SA, Yahyazadehfar M. Synthesis and characterization of CO-MOF@ Ag2O nanocomposite and its application as a nano-organic catalyst for one-pot synthesis of pyrazolopyranopyrimidines. Sci Rep. 2023;13:17500.
47. Diamond BG, Payne LI, Hendon CH. Ligand field tuning of d-orbital energies in metal-organic framework clusters. Commun Chem. 2023;6:67.
48. Ding M, Cai X, Jiang HL. Improving MOF stability: approaches and applications. Chem Sci [Internet]. 2019;10:10209–30. Available from: https://doi.org/10.1039/C9SC03916C
49. Usman M, Khan RA, Alsalme A, Alharbi W, Alharbi KH, Jaafar MH, et al. Structural, Spectroscopic, and Chemical Bonding Analysis of Zn(II) Complex [Zn(sal)](H2O): Combined Experimental and Theoretical (NBO, QTAIM, and ELF) Investigation. Crystals (Basel) [Internet]. 2020;10:259. Available from: https://doi.org/10.3390/cryst10040259
50. Miar M, Shiroudi A, Pourshamsian K, Oliaey AR, Hatamjafari F. Theoretical investigations on the HOMO–LUMO gap and global reactivity descriptor studies, natural bond orbital, and nucleus-independent chemical shifts analyses of 3-phenylbenzo[*d*]thiazole-2(3 *H*)-imine and its *para* -substituted derivatives: Solvent and substituent effects. J Chem Res [Internet]. 2021;45:147–58. Available from: https://doi.org/10.1177/1747519820932091
51. Gounhalli SG, Basavaraj S, Hanagodimath SM. Spectroscopic analysis of NMR, IR, Raman and UV-Visible, HOMO-LUMO, ESP and Mulliken charges of coumarin derivative by density functional theory. Journal of the Maharaja Sayajirao University of Baroda ISSN. 2021;25:0422.
52. Vaishampayan A, Grohmann E. Antimicrobials Functioning through ROS-Mediated Mechanisms: Current Insights. Microorganisms [Internet]. 2021;10:61. Available from: https://doi.org/10.3390/microorganisms10010061
53. Atlaw A, Kebede HB, Abdela AA, Woldeamanuel Y. Bacterial isolates from diabetic foot ulcers and their antimicrobial resistance profile from selected hospitals in Addis Ababa, Ethiopia. Front Endocrinol (Lausanne). 2022;13:987487.
54. Adeyemo AT, Kolawole B, Rotimi VO, Aboderin AO. Multicentre study of the burden of multidrug-resistant bacteria in the aetiology of infected diabetic foot ulcers. Afr J Lab Med [Internet]. 2021;10:1–10. Available from: https://doi.org/10.4102/ajlm.v10i1.1261
55. Barrigah-Benissan K, Ory J, Dunyach-Remy C, Pouget C, Lavigne JP, Sotto A. Antibiofilm properties of antiseptic agents used on Pseudomonas aeruginosa isolated from diabetic foot ulcers. Int J Mol Sci. 2022;23:11270.
56. Stańkowska M, Garbacz K, Korzon-Burakowska A, Bronk M, Skotarczak M, Szymańska-Dubowik A. Microbiological, Clinical and Radiological Aspects of Diabetic Foot Ulcers Infected with Methicillin-Resistant and -Sensitive Staphylococcus aureus. Pathogens [Internet]. 2022;11:701. Available from: https://doi.org/10.3390/pathogens11060701
57. Liu Y, Zhou L, Dong Y, Wang R, Pan Y, Zhuang S, et al. Recent developments on MOF-based platforms for antibacterial therapy. RSC Med Chem. 2021;12:915–28.
58. Elmehrath S, Ahsan K, Munawar N, Alzamly A, Nguyen HL, Greish Y. Antibacterial efficacy of copper-based metal–organic frameworks against Escherichia coli and Lactobacillus. RSC Adv. 2024;14:15821–31.
59. Bhardwaj N, Pandey SK, Mehta J, Bhardwaj SK, Kim KH, Deep A. Bioactive nano-metal–organic frameworks as antimicrobials against Gram-positive and Gram-negative bacteria. Toxicol Res (Camb) [Internet]. 2018;7:931–41. Available from: https://doi.org/10.1039/C8TX00087E